

Numerical Investigation of Heat Transfer Enhancement of Turbulent Flow in Dimpled Tubes

Elhassen Ali Ahmed Omer¹ , Ali Ali Khalifa Alkharboushi^{1*}

¹ Mechanical Engineering Department, Faculty of Engineering, University of Zawia, Zawia, Libya.

*Corresponding author email: a.alkharboushi@zu.edu.ly

Received: 11.11.2023 | Accepted: 07.12.2023 | Available online: 15-12-2023 | DOI:10.26629/uzjest.2023.08

ABSTRACT

The importance of heat transfer enhancement has gained greater significance in many engineering applications, and a great amount of effort has been devoted to the use different techniques to improve the thermal performance of flowing fluids in pipes. Dimpled tubes were used for this purpose in this study. In this investigation, the heat transfer-flow characteristics of turbulent flow in dimpled tubes subjected to uniform heat flux are numerically investigated. The rate of heat transfer, friction factor, and performance evaluation criterion were determined for various designs of dimpled tubes and compared with smooth tubes. The considered cases are conducted in the Reynolds number range of 3000 to 12,000. The ANSYS Fluent R19 is used for this purpose. The Reynolds-averaged Navier-Stokes equations (RANS) are used to model the governing flow equations. The realizable $k-\epsilon$ turbulence model is used with enhanced wall conditions to simulate turbulent flow adjacent to the inner wall surface. The results revealed that the rate of heat exchange in dimpled tubes higher than that of smooth ones. but with additional pressure loss. Moreover, the heat transfer performance of the staggered arrangement is higher than the inline arrangement by 17 %. Also, the performance evaluation criteria (PEC) increases with the increasing in dimples diameter, and decreases with increasing in relative pitch spacing, the maximum enhancement reaches 31% for $d = 5$ mm, and relative pitch spacing $S/D = 2$ at $Re = 4000$.

Keywords: Dimple tube, turbulent flow, heat transfer enhancement – Nusselt number

دراسة عددية لتعزيز انتقال الحرارة للتدفق المضطرب في الأنابيب المدملة

الحسن علي أحمد عمرو¹ ، علي علي خليفة الخربوشي¹

¹ قسم الهندسة الميكانيكية والصناعية، كلية الهندسة جامعة الزاوية، الزاوية، ليبيا.

ملخص البحث

نظرا لأهمية انتقال الحرارة وتحسينها في العديد من الاستخدامات الهندسية وتوجه الباحثون لاستخدام التقنيات المختلفة لتحسين انتقال الحرارة. تم في هذا البحث دراسة تحليلية لتعزيز أداء انتقال الحرارة للتدفق المضطرب داخل الأنابيب المدملة بواسطة برنامج ANSYS Fluent R19. تم استخدام معادلات رينولدز المتوسطة لمعادلات نافير-ستوكس ونموذج $k-\epsilon$ للتدفق المضطرب. وقد تم تغيير رقم رينولدز بين 3000 – 12000. وكانت ظروف التسخين بثبوت

الفيض الحراري عند 5000 W/m^2 . لدراسة تأثير الدمامل بالأنايبب تمت دراسة عدة عوامل وهي القطر والمسافة الفاصلة وترتيب الدمامل، ومقارنة أدائها الحراري مع الأنبوب الأملس. وأظهرت النتائج أن الأداء الحراري للأنايبب متخالفة الدمامل أفضل ب 17% من الأنايبب المتناظرة الندب عند مقارنتها بالأنبوب الأملس. وبالتالي استخدمت لدراسة تأثير باقي العوامل. وبينت النتائج التحليلية تحسن عدد نسلت وبالتالي انتقال الحرارة بنسبة 15% عند استخدام أنبوب بقطر أكبر. واستخدم القطر الأكبر لدراسة تأثير المسافة الفاصلة بين الندب S/D بنسب مختلفة وأوضحت النتائج أفضلية الأداء الحراري للمسافة الأقصر. واستخدمت نسبة التحسين الكلية للمقارنة بين حالات نماذج البحث المختلفة وتبين أن الانبوب المدمل يعطي أداءً حرارياً مقارنًا مع الأنبوب الأملس.

الكلمات الدالة: الأنايبب المدملة - التدفق المضطرب - تحسين انتقال الحرارة - رقم نسلت.

1. Introduction

Heat exchangers are employed in many engineering applications, such as power plants, heat recovery units, the food industry, aviation and nuclear reactors. Hence, it is significant to select appropriate improved methods to decrease the size and enhance the thermal performance of these devices and reduce their costs [1].

Heat transfer augmentation can be divided into three main categories. Namely, the active approach that requires an external power input, such as electric energy; the passive approach that deals with modified surfaces; and a combined approach where advantages of the active and passive methods are combined. Passive methods have attracted the largest attention among researchers due to the fact that there is no additional power input required to achieve the heat transfer enhancement [2]. One method of enhancing tube convective heat transfer is to limit the growth of the thermal boundary layer associated with turbulent flow inside the tube. The thermal boundary layer can be made thinner or partially broken by flow disturbance. Disruption of the laminar sublayer in the turbulent boundary layer is an effective method for augmenting heat transfer. Using dimples on the pipe surface is a passive technique for enhancing the heat transfer characteristics of a pipe. Dimples may be provided on the outer or inner side of the tube. Their effects can be varied by changing their dimple shapes, orientations, and depths. The dimples in the pipe essentially have a tripping effect on the fluid flow leading to an increase in the mixing of the fluid and reducing the growth of the thermal boundary layer. However, it is commonly observed that implementing these techniques may often lead to pressure drops, so an optimum design is always required. Many researchers have investigated the effects of various geometries of dimples on heat performance experimentally and numerically to quantify the heat exchange enhancement using surface modified tubes. Modest increases in pressure drop in these tubes were also observed.

In an experimental work of [3], the effect of dimples shape and pitch on the heat transfer rate in dimpled channels were tested at different flow conditions. The results reveal that the diameter and the pitch have a significant effect on thermal performance; the outcomes gave the maximum enhancement in Nusselt number of 3.94 compared to the plane channel was achieved. Many have investigated numerically and experimentally the effect of dimples on the performance of heat exchangers with various dimensions and arrangements at different water flow rates as the working fluid. The results show that the overall heat transfer coefficient of the concentric dimple tube heat exchanger increased from 56% to 64% as compared with the concentric plain tube heat exchanger [4–6]. The enhancement of heat transfer and corresponding pressure drop in an inside deeply dimpled enhanced tube was investigated numerically. The effect of various dimple diameters, pitches and dimple heights on the heat transfer and flow characteristics inside the deeply dimpled tube. All results showed that the Nu number increased with the use of dimples and a higher performance enhancement was obtained. Also, transverse and longitudinal dimples improved flow mixing inducing swirl flows and an interrupted boundary layer,

thus improving heat transfer rates [7–9]. Comparisons of different shapes of dimples in tubes were studied numerically [10]. The analysis used a tube named ETTD (enhanced tubes with teardrop dimples) and concluded that the teardrop had better heat transfer and a lower pressure drop compared with the spherical and elliptical dimple tubes.

Thus, the current study examines turbulent forced convective flow in a dimpled tube with different arrangements and dimensions. The flow is considered turbulent and the Reynolds numbers are in the range of $3,000 \leq Re \leq 12,000$ under a constant heat flux condition. Results of interest including the average Nusselt number, pressure drop (Δp), and performance evaluation criteria (PEC).

2. Physical and Mathematical Modelling

The computational domain is created as a three dimensional tube with an internal diameter of D , a dimple diameter of d , and a pitch spacing S . The overall length of the channel was 1100 mm, the test section length (L) was 600 mm, and for ensuring fully developed flow at the test part, the upstream or entrance section length (L_i) was 150 mm. Also, downstream exit section length (L_e) of 350 mm is needed to prevent the opposite flow that could affect the accuracy of the computation. In addition, a uniform heat flux prescribed at the test section of 5000 W/m^2 . The tube diameter (D) is 20 mm, and different dimples diameters and pitch spacing between dimples will be investigated. A schematic diagram of the tube specifications and computational domain are shown in Figure 1 and 2 respectively.

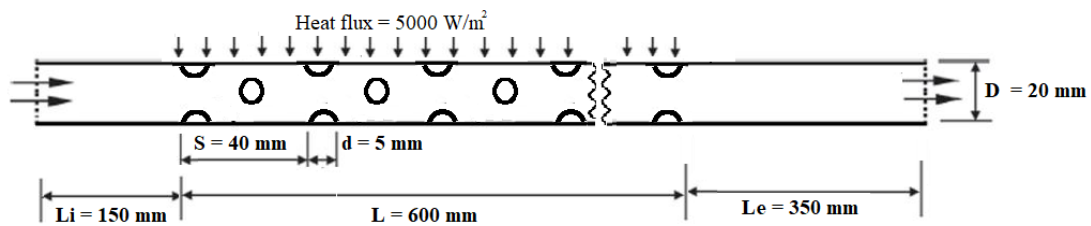


Figure 1. Schematic diagram of tube specifications and dimensions

2.1. The governing equations

The flow under consideration is governed by the incompressible, steady form of continuity, the time-averaged Navier–Stokes equations and the energy equation. Viscous dissipation, natural convection and radiation heat transfer effects are discarded. In the Cartesian system, these equations can be written as [11]:

$$\frac{\partial}{\partial x_i} (\rho u_i) = 0 \quad (1)$$

$$\frac{\partial}{\partial x_j} (\rho u_j u_i) = -\frac{\partial p}{\partial x_i} + \frac{\partial}{\partial x_j} \left[\mu \left(\frac{\partial u_i}{\partial x_j} + \frac{\partial u_j}{\partial x_i} \right) \right] + \frac{\partial}{\partial x_j} (-\rho \overline{u'_i u'_j}) \quad (2)$$

$$\frac{\partial}{\partial x_j} [u_i (\rho T)] = \frac{\partial}{\partial x_j} \left[\left(\frac{\mu}{Pr} + \frac{\mu_t}{Pr_t} \right) \frac{\partial T}{\partial x_i} \right] \quad (3)$$

where p is the pressure, (Pa), u is the velocity component, u' is the velocity fluctuations, (m/s), x is the spatial coordinates, (m), Pr is the Prandtl number, Pr_t is the turbulent Prandtl number, T is the temperature, (K), ρ is the density, (kg/m^3), μ is the dynamic viscosity and μ_t is the turbulent dynamic viscosity, (N s/m^2).

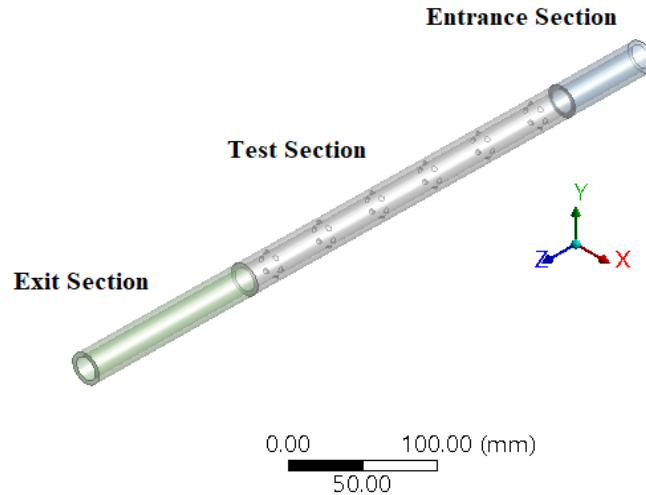


Figure 2. The computational domain

The normal Reynolds stress, which is combined by the Boussinesq relationship and the eddy viscosity is given by:

$$-\rho \overline{u'_i u'_j} = \mu_t \left(\frac{\partial u_i}{\partial x_j} + \frac{\partial u_j}{\partial x_i} \right) \quad (4)$$

The standard k- ϵ is the most common model used in Computational Fluid Dynamics (CFD) for the solution of practical engineering flow problems. It is a two equation model which gives a general description of turbulence by means of two transport equations. The turbulence turbulent kinetic energy (κ) and the turbulent kinetic energy dissipated (ϵ) equations are given as [12]:

$$\frac{\partial}{\partial x_i} [\rho k u_i] = \frac{\partial}{\partial x_j} \left[\left(\mu + \frac{\mu_t}{\sigma_k} \right) \frac{\partial k}{\partial x_j} \right] - \rho \overline{u'_i u'_j} \frac{\partial u_j}{\partial x_i} - \rho \epsilon \quad (5)$$

$$\frac{\partial}{\partial x_i} [\rho \epsilon u_i] = \frac{\partial}{\partial x_j} \left[\left(\mu + \frac{\mu_t}{\sigma_\epsilon} \right) \frac{\partial \epsilon}{\partial x_j} \right] - C_{1\epsilon} (\epsilon/k) \rho \overline{u'_i u'_j} \frac{\partial u_j}{\partial x_i} - C_{2\epsilon} \rho (\epsilon^2/k) \quad (6)$$

The turbulent viscosity, which is expressed as:

$$\mu_t = \rho C_\mu k^2 / \epsilon \quad (7)$$

The empirical constants for the turbulent model are:

$C_\mu = 0.09$; $\sigma_k = 1.0$; $\sigma_\epsilon = 1.3$; $C_{1\epsilon} = 1.47$; $C_{2\epsilon} = 1.92$; and $Pr_t = 0.85$.

2.2. Boundary conditions

Since the governing equations are in spatial coordinates, boundary conditions were provided for all boundaries of the computation domain. The descriptions of different boundary conditions are given as follows:

1. Uniform axial velocity corresponding to the range of $3,000 \leq Re \leq 12,000$ and temperature of 300 K assigned at the inlet section of flowing water. The turbulent kinetic energy (k_{in}) and the turbulent dissipation (ϵ_{in}) are calculated accordingly.
2. No-slip condition is considered at the tube wall. The heat transfer section has the prescribed heat flux of 5000 W/m^2 at the test section.
3. At the entrance and in extended regions, adiabatic conditions were assumed.

4. The pressure outlet boundary condition is applied to the outlet because the ambient pressure is prevailing there. Also, it is assumed that all variables have negligible stream-wise gradients.

2.3. Parameter definitions

In order to present the results of the numerical solution, the parameters employed in the investigation are now described, to analyze the flow characteristics and the pressure drop in a pipe for turbulent conditions, the Reynolds number (Re) and the friction factor are defined as [13]:

$$Re = \frac{\rho u_{in} D}{\mu} \quad (8)$$

$$f = 2 \frac{\Delta p}{L} \frac{D}{\rho u_{in}^2} \quad (9)$$

where u_{in} is the inlet velocity, (m/s), D is the tube diameter, (m), ρ is the density, (kg/m^3), μ is the dynamic viscosity, (kg/ms), Δp is the pressure drop, (Pa) and L is the test section length, (m).

The local convective heat transfer coefficient and the mean Nusselt number are determined by [14]:

$$h_x = \frac{q}{T_w - T_f(x)} \quad (10)$$

$$Nu_m = \frac{D}{\lambda} \int_L h_x dx \quad (11)$$

where q_w is the prescribed heat flux on the wall, (W/m^2), λ is the thermal conductivity of the flowing fluid, (W/mK), T_w is the area-weighted average temperature of the internal wall and T_f is the cross-section mass-weighted average temperature of the fluid.

For a better evaluation system, the performance evaluation criterion (PEC) was computed to simultaneously examine the thermal performance of the dimpled tube, based on the ratio between the heat transfer enhancement and the increase in the friction factor. It is defined under the same pumping power as follows [15]:

$$PEC = \left(\frac{Nu}{Nu_0} \right) / \left(\frac{f}{f_0} \right)^{1/3} \quad (12)$$

where Nu is the Nusselt number, Nu_0 is the Nusselt number for a smooth tube, f is the friction factor and f_0 is the friction factor for a smooth tube.

3. Numerical Solution

For the purpose of solving turbulent flow and heat transfer, the governing equations with corresponding boundary conditions are solved using the finite volume method, which is employed by implementing the CFD commercial software ANSYS-FLUENT-V 19. The pressure-based model with the SIMPLE algorithm was employed for the pressure-velocity fields and a second-order upwind scheme was utilized for the equations of momentum, turbulence kinetic energy and turbulence dissipation rate. The realizable $k-\varepsilon$ model with enhanced wall treatment is adopted because it can provide improved predictions of near-wall flows. The discretized algebraic finite volume equations have been solved iteratively and residuals have been reduced to a value 10^{-6} . The number of iterations is set to 5000, and calculations start. The iterations continue until the convergence is reached. Figure 3 shows an example of a hybrid unstructured grid for the computational domain. The grids near the solid wall are very dense to ensure the near-wall y^+ value, for $y^+ \approx 1$ to provide better resolution of the viscous effects in the boundary layers, while the grid density is relatively sparse far from the boundary [16].

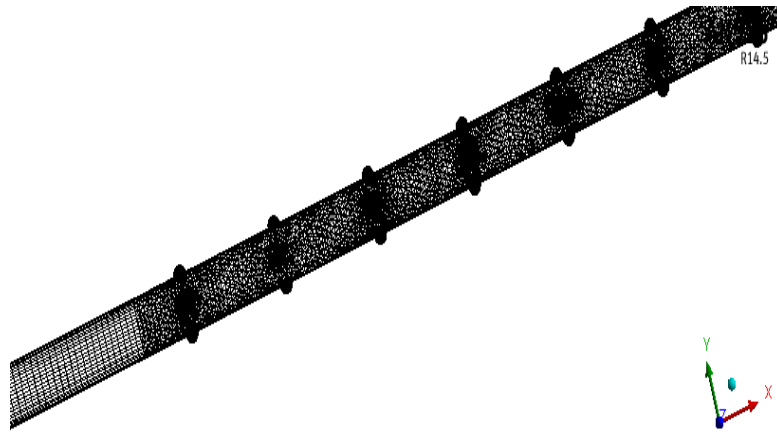


Figure 3. The computational mesh.

4. Grid Independence Test and Model Validation

To ensure the accuracy and validity of the numerical results, a mesh independence study was carried out for Re in the staggered case with $d = 5$ mm and $S/D = 2$. Initially, a coarse grid of 89,673 cells was used, and then the number of cells increased to 206,382. By doing this, the mean Nu number has increased by 32.8 %. When the cell number increased to 273,786, a small change in the Nusselt number of less than 1% was obtained. The results of this test is shown in Figure 4. Therefore, the domain with 206,382 cells is used in our testing computations.

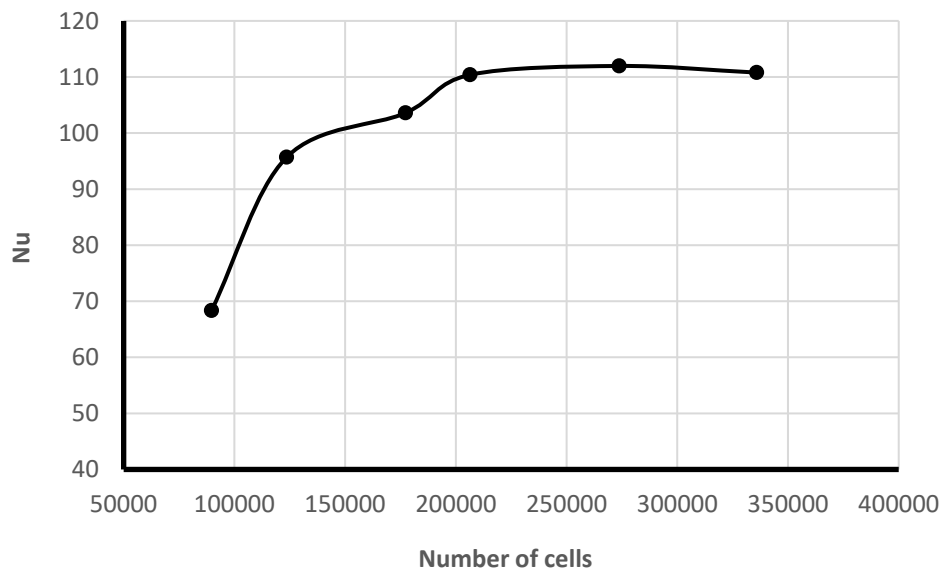


Figure 4. Grid independence test.

For validation, Figure 5 shows the comparisons of numerical simulation and calculation results of the Nusselt number between the present study and Dittus-Boelter correlations [17]. The deviation between the numerical results and the related results of Dittus-Boelter is less than 2%.

5. Results and discussion

The effect of dimple arrangement, dimple diameters and relative dimple spacing on heat transfer enhancement and flow in dimpled pipes was investigated. The simulations were conducted under turbulent conditions ranging from $3,000 \leq Re \leq 12,000$, and the test section was subjected to a uniform heat flux of 5000 W/m^2 . The testing cases are:

- The dimple arrangements: inline and staggered.

- The dimple diameter: 3, 4 and 5 mm.
- The relative pitch spacing, which is the ratio (S/D) varied as 2, 3.5 and 5.

The results have been presented and discussed in this section.

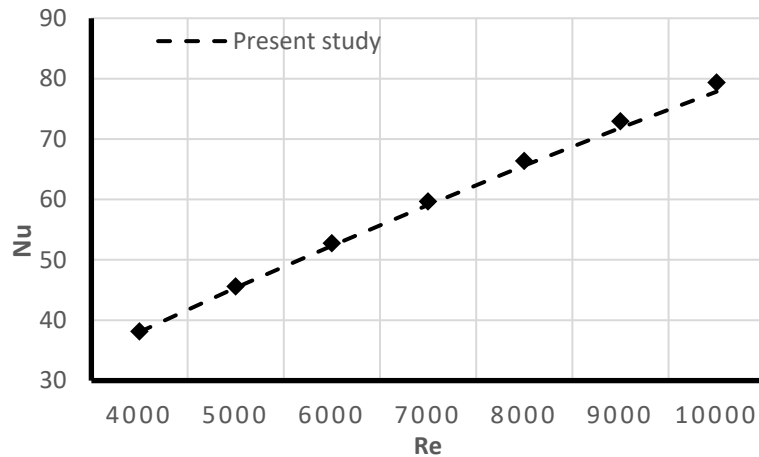


Figure 5. Validation of the Nusselt number

5.1. Effect of dimples arrangement

Two arrangements of dimples placed along the tube surface were investigated; the inline and staggered dimples arrangements. The test was carried out at constant dimple diameter and pitch ratio $S/D = 2$, all with approximately the same number of dimples.

The test results presented in Figure 6 show that the Nusselt number increases with increasing Reynolds number as for the conventional turbulent flow in tubes. Also, the results reveal that the heat transfer performance of the staggered arrangement is higher than the inline one by 17 %. This is due the higher turbulence intensity and vortex formation induced in the flow field in the staggered arrangement. Therefore, the staggered arrangement is adopted to investigate other factors in dimpled tubes.

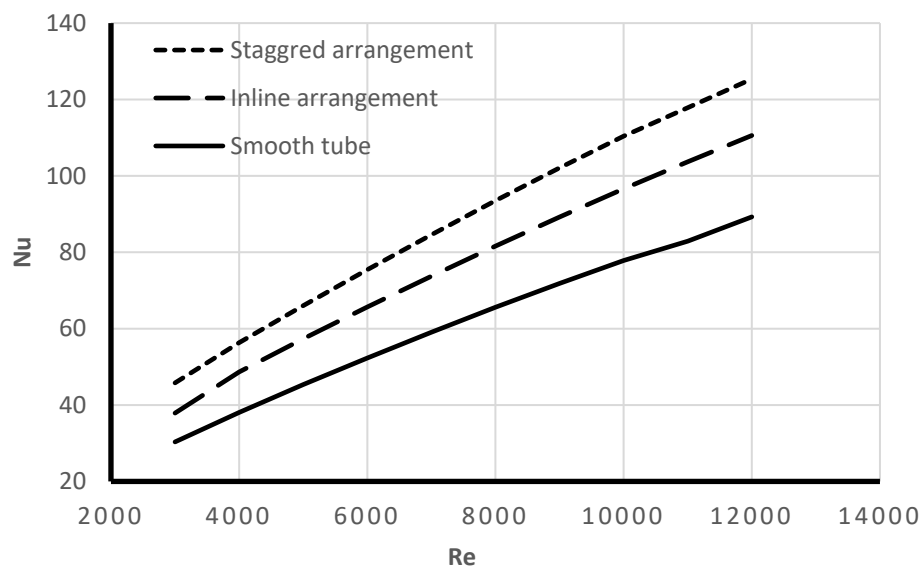


Figure 6. Effect of dimple arrangement on heat transfer

5.2. Effect of dimple diameter

Figure 7 shows the effect of the Reynolds number on the Nusselt number under different dimple diameters. The effect of different diameters (3mm, 4mm and 5mm) and constant pitch spacing ($S/D = 2$). The Nusselt number investigations are performed in a dimpled tube with the Reynolds number ranging from 3000 to 12000.

The results showed that the Nusselt number increases gradually with the increasing Reynolds number for all the smooth and dimpled tubes. And for the same Reynolds number, all the dimpled tubes has a higher Nusselt number than the smooth tube. Also, the Nusselt number gradually increases as the radius of the spherical dimple increases. This enhancement in heat transfer due to the large dimple diameter makes the kinetic energy of the core flow dominant and much higher than the shear force induced by the dimpled surface. Therefore, different diameters or different heights of the dimple (1.5 mm, 2 mm, and 2.5 mm) caused an increase in mixing between the secondary and core flows, consequently, the local heat transfer on the tube wall will be improved.

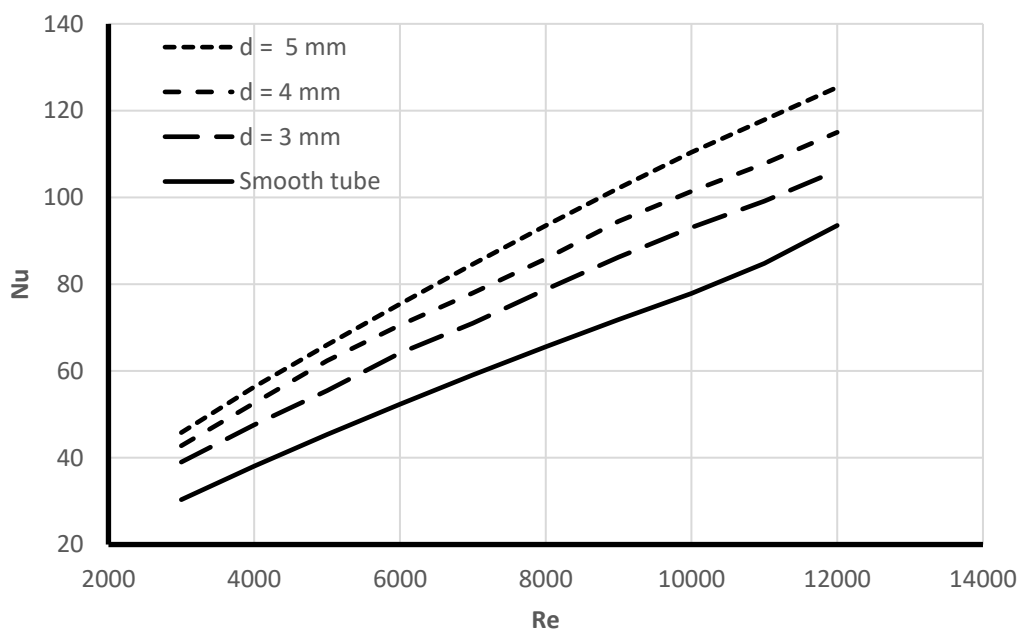


Figure 7. Effect of dimple diameter on heat transfer

Figure 8 shows the friction factor values versus the Reynolds number for the cases of smooth and dimpled tubes with different dimple diameters. It presents the friction factor compared to a smooth tube with the same hydraulic diameter and length. Generally, the friction factor decreases as the Reynolds number increases. The friction factor gives an idea of the needed pumping power input. Placed dimples on the tube surface work as an obstacle in the direction of the flow; therefore, the friction factor is higher for the dimpled tubes, pressure drop increases and more pumping power input is needed to pump the fluid.

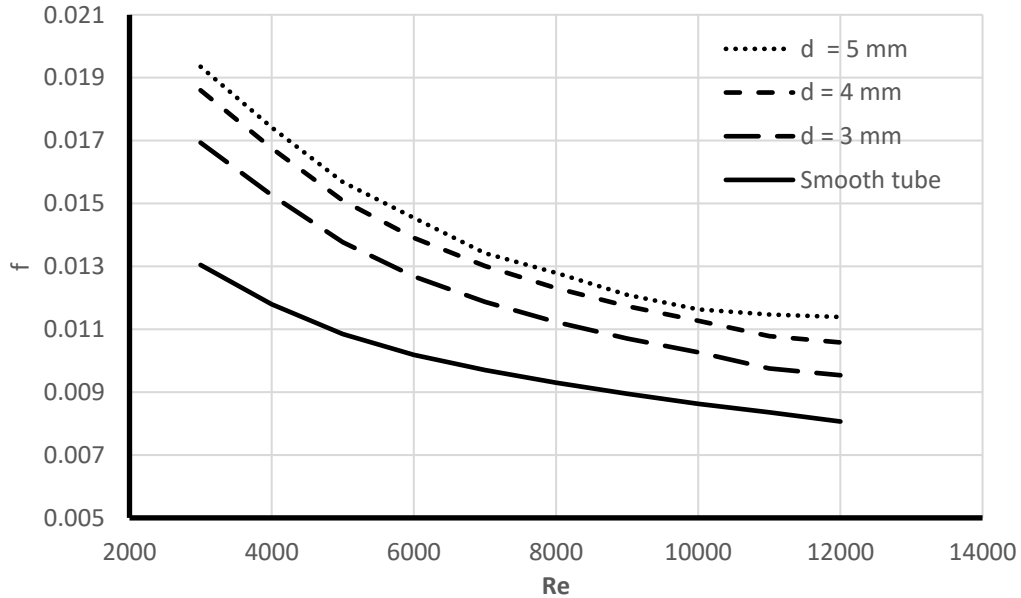


Figure 8. Effect of dimple diameter on friction factor

The performance evaluation criteria (PEC) were used to compare the overall performance of the dimpled tubes. The PEC results for different dimple diameters are plotted in Figure 9. It can be seen that compared with smooth tubes, the PEC is higher than one for all configurations. According to the definition, higher values than one ensure better heat transfer enhancement against the pressure drop penalty.

As can be seen in this figure, with an increase in the Reynolds number, PEC magnitudes decrease. The reason for this result is that friction factor results are dominated by the Nusselt number, and the friction factor results are much more than smooth tube results.

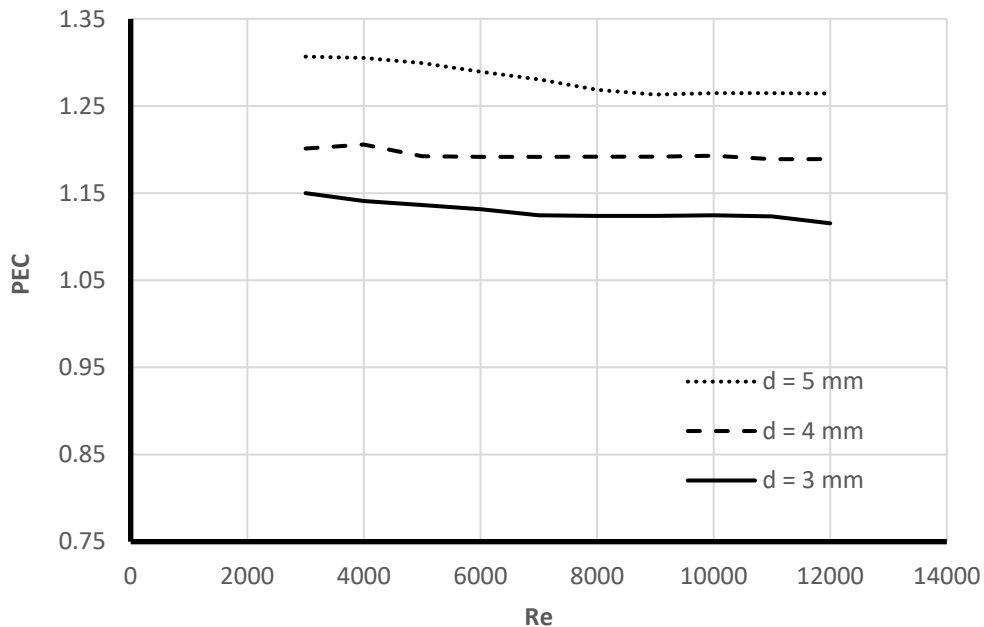


Figure 9. The performance evaluation criterion for different dimple diameters

5.3. Effect of dimple spacing

Figure 10 presents the distribution of the Nusselt number for different pitch-to-pipe diameter ratios (S/D), for the dimple diameter of 5 mm in a staggered arrangement. Generally, heat transfer increases with increasing Reynolds number. The results of all cases of different pitch lengths show this behavior. Also, it can be noticed that as the pitch length decreases, the Nusselt number increases at the same Reynolds number. Decreasing the pitch length of the dimpled means increasing the number of dimples. Therefore, it causes more turbulence in the dimpled tube and enhances heat transfer. The more dimples there are, the more turbulent it becomes especially near the inner surface of the wall. Generally, the friction factor decreases as the Reynolds number increases.

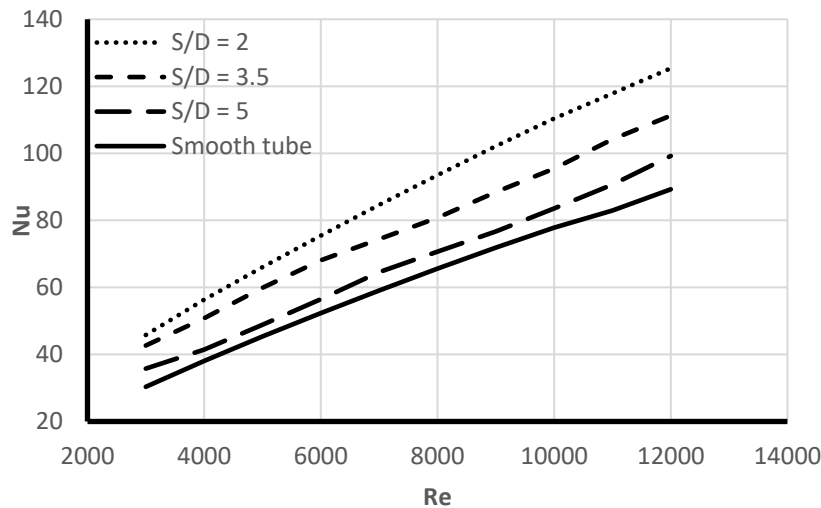


Figure 10. Effect of dimple spacing on heat transfer

Figure 11 shows the friction factor values versus the Reynolds number for the cases of smooth and dimpled tubes with different dimple relative pitches. It presents the friction factor compared to a smooth tube with the same hydraulic and dimple diameter. The results showed that as the pitch length increases, the friction factor decreases at the same Reynolds number. This can be explained by the fact that as the pitch length increases, fewer number of dimples cover the tube surface, so it would decrease the number of induced vortexes along the tube, causing a lesser friction factor in a specific Reynolds number.

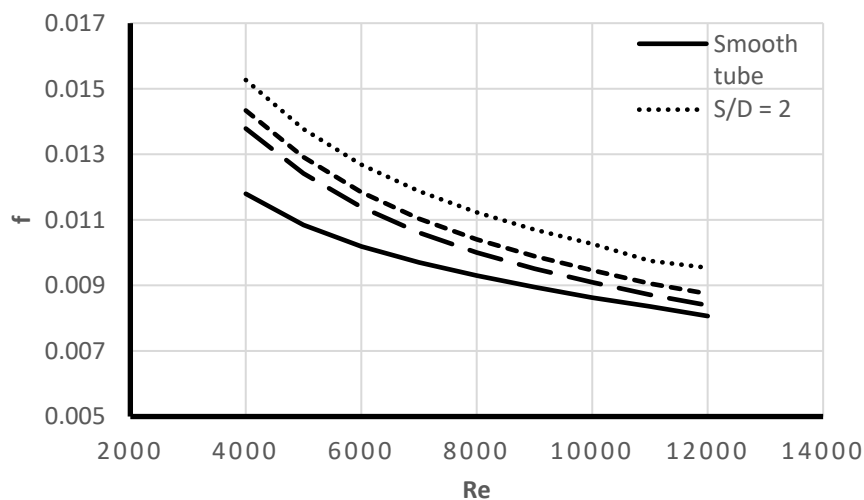


Figure 11. Effect of dimple spacing on friction factor

Figure 12 demonstrates the variation of PEC against the Reynolds number with various pitch spacing ratios. Evidently, the PEC values of dimpled tubes were greater than those of smooth pipes. This is because the thermal performance factor depends on the heat transfer enhancement, which can be

deduced from enhanced Nu results. But the Re has an opposite effect, where the PEC decreases as the Re increases.

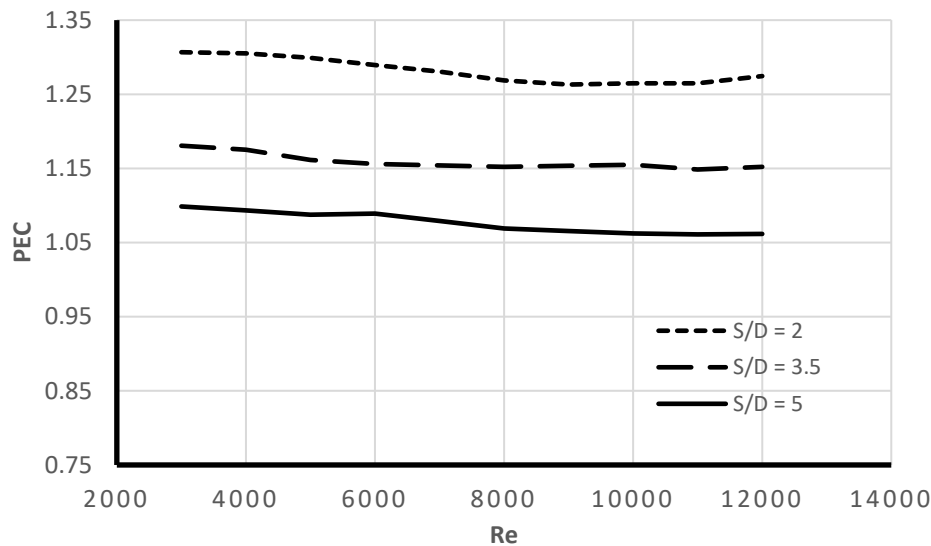


Figure 12. The performance evaluation criterion for different dimple spacing.

6. Conclusions

In this study, the heat transfer enhancement and flow through a horizontal tube under constant heat flux and turbulent flow conditions ($3,000 \leq Re \leq 12,000$) are numerically investigated. The influences of the dimpled arrangements, dimple diameter and pitch length between the dimple rows on the heat transfer rate and friction factor characteristics have been investigated. The major conclusion of this numerical study is that the utilization of dimples on tubes can be offered as an appropriate technique to improve thermal performance, which can prompt the design plan of heat exchangers and make them more compact. Over a range of Re numbers investigated tubes with dimples have a higher Nusselt number and friction factor in comparison with smooth plain tubes. Staggered arrangements of dimpled tube manifested a better enhancement of heat transfer by 17% than Inline arrangement at the same dimples diameters and relative pitch ratio. The Nusselt number and the friction factor increase as dimple diameter increases and relative pitch (S/D) decreases. The PEC increases with the increases in the dimples diameter, and decreases with the increase of relative pitch spacing. The enhancement reaches 31% for $d = 5$ mm and $S/D = 2$.

REFERENCES

- [1] Ajarostaghi, S.S., Zaboli, M., Javadi, H., Badenes, B., Urchueguia, J.F., A Review of Recent Passive Heat Transfer Enhancement Methods, *Energies*, 2022, 15, 986.
- [2] Singh, P. Navin Kumar, N., Review of Heat Transfer Enhancement Methods, *Int. Journal of Research Publication and Reviews*, 2022, vol 3, no 6, pp. 2247-2252.
- [3] Reddy, M., Nusselt number and friction factor correlations of three sides concave dimple roughened solar air heater, *Renewable Energy*, 2019, vol.135, pp. 355-377.
- [4] Babu, J.S. and Sellamuthu, P., Analysis of heat transfer and fluid flow characteristics of concentric tube heat exchanger with dimpled tube, *Journal of Xi'an University of Architecture & Technology*, 2020, vol. XII, no. VIII, pp. 508–516.
- [5] Ying, P.; He, Y.; Tang, H.; Ren, Y., Numerical and Experimental Investigation of Flow and Heat Transfer in Heat Exchanger Channels with Different Dimples Geometries, *Machines*, 2021, 9, 72.
- [6] Gupta, G., Fernandez, E., Otto, M., and Kapat, J. S., Experimental and numerical investigation of fully turbulent flow in a rectangular channel with dimples and protrusions, *In AIAA Propulsion and Energy Forum*, 2019, vol. 68, pp. 4178-4194.

- [7] Babu, H.S., Midhun K. R., Ajeesh, C. P., Raj, A., Murali, K.K., Effect of dimples on flow performance of enhanced surface tubes, *Int. Res. J. of Engg. and Tech. (IRJET)*, 2023, vol. 10, no. 10, pp. 569 – 578.
- [8] Cheraghi, M. H., Ameri, M. and Shahabadi. M., Numerical study on the heat transfer enhancement and pressure drop inside deep dimpled tubes, *Int. J. of Heat and Mass Transfer*, 2020, vol. 147, pp. 458 – 467.
- [9] Liu J., Chen S., Gan M., Chen Q., Heat Transfer and Flow characteristics inside an Innovative Vortex Enhanced Tube, *App. Therm. Engg*, 2018, vol. 12, pp. 120–150.
- [10] Xie, S., Liang, Z., Zhang, L., Wang, Y., Ding, H., Numerical investigation on flow and heat transfer in dimpled tube with teardrop dimples, *Int. J. Heat Mass Transfer*, 2019, vol. 131, no. 3, pp. 713–723.
- [11] Davidson, L, Fluid mechanics, turbulent flow and turbulence modeling, Division of Fluid Dynamics, Department of Mechanics and Maritime Sciences, *Chalmers University of Technology*, Goteborg, Sweden, 2022.
- [12] Tokgoz1, N., Aliç, E. , Kaşka, Ö., Aksoy, M. M., The numerical study of heat transfer enhancement using AL2O3- water nanofluid in corrugated duct applications, *J. of Thermal Engg*, 2018, vol. 4, mo. 3, pp. 1984–1997.
- [13] Sun, H., Fu, H., Yan, L., Ma, H., Luan, Y., Magagnato, F., Numerical Investigation of Flow and Heat Transfer in Rectangular Microchannels with and without Semi-Elliptical Protrusions, *Energies* 2022, vol.15, 4927.
- [14] Huang, Z. , Yu, G.L., Lia, Z.Y., Tao, W.Q., Numerical study on heat transfer enhancement in a receiver tube of parabolic trough solar collector with dimples, protrusions and helical fins, *Energy Procedia*, 2015, vol. 69, pp. 1306 – 1316.
- [15] Ajeel, R.K., Salim, W.I., Hasnan, K., Thermal and hydraulic characteristics of turbulent nanofluids flow in trapezoidal corrugated channel: symmetry and zigzag shaped, *Therm. Engg...*, 2018, vol. 1, no, 12 pp. 620–635.
- [16] ANSYS FLUENT THEORY GUIDE, RELEASE 19.0.; ANSYS, Inc, PA, USA, 2019.
- [17] Bergman, T. Lavine, A. Incropera, F. and Dewitt, D., FUNDAMENTALS OF MASS AND HEAT TRANSFER, 6th ed., John Wiley & Sons, USA, 2007, pp. 486-534.